ISSN 1674-1056
http://cpb.iphy.ac.cn
http://iopscience.iop.org/cpb
中国物理 B
Chinese Physics
中国物理 Chinese Physics B

Single-channel vector magnetic information detection method based on diamond NV color center

Qin-Qin Wang(王琴琴), Rui-Rong Wang(王瑞荣), Jin-Ping Liu(刘金萍), Shao-Zhuo Lin(林绍卓), Liang-Wei Wu(武亮伟), Hao Guo(郭浩), Zhong-Hao Li(李中豪), Huan-Fei Wen(温焕飞), Jun Tang(唐军), Zong-Min Ma(马宗敏), and Jun Liu (刘俊)

Citation: Chin. Phys. B, 2021, 30 (**8**): 080701. DOI: 10.1088/1674-1056/abea84
Journal homepage: http://cpb.iphy.ac.cn; http://iopscience.iop.org/cpb

What follows is a list of articles you may be interested in

Magnetic shielding property for cylinder with circular, square, and equilateral triangle holes

Si-Yuan Hao(郝思源), Xiao-Ping Lou(娄小平), Jing Zhu(祝静), Guang-Wei Chen(陈广伟), and Hui-Yu Li(李慧宇)
Chin. Phys. B, 2021, 30 (**6**): 060702. DOI: 10.1088/1674-1056/abeeee

A modified analytical model of the alkali-metal atomic magnetometer employing longitudinal carrier field

Chang Chen(陈畅), Yi Zhang(张燚), Zhi-Guo Wang(汪之国), Qi-Yuan Jiang(江奇渊), Hui Luo(罗晖), and Kai-Yong Yang(杨开勇)
Chin. Phys. B, 2021, 30 (**5**): 050707. DOI: 10.1088/1674-1056/abd7d3

Search for topological defect of axionlike model with cesium atomic comagnetometer

Yucheng Yang(杨雨成), Teng Wu(吴腾), Jianwei Zhang(张建玮), and Hong Guo(郭弘)
Chin. Phys. B, 2021, 30 (**5**): 050704. DOI: 10.1088/1674-1056/abf132

Atomic magnetometer with microfabricated vapor cells based on coherent population trapping

Xiaojie Li(李晓杰), Yue Shi(史越), Hongbo Xue(薛洪波), Yong Ruan(阮勇), and Yanying Feng(冯焱颖)
Chin. Phys. B, 2021, 30 (**3**): 030701. DOI: 10.1088/1674-1056/abc2b9

A slope-based decoupling algorithm to simultaneously control dual deformable mirrors in a woofer-tweeter adaptive optics system

Tao Cheng(程涛), Wenjin Liu(刘文劲), Boqing Pang(庞博清), Ping Yang(杨平), Bing Xu(许冰)
Chin. Phys. B, 2018, 27 (**7**): 070704. DOI: 10.1088/1674-1056/27/7/070704

Single-channel vector magnetic information detection method based on diamond NV color center*

Qin-Qin Wang(王琴琴), Rui-Rong Wang(王瑞荣), Jin-Ping Liu(刘金萍), Shao-Zhuo Lin(林绍卓), Liang-Wei Wu(武亮伟), Hao Guo(郭浩)†, Zhong-Hao Li(李中豪), Huan-Fei Wen(温焕飞), Jun Tang(唐军)‡, Zong-Min Ma(马宗敏), and Jun Liu (刘俊)§

Key Laboratory of Instrumentation Science and Dynamic Measurement, School of Instrument and Electronics, North University of China, Taiyuan 030051, *China*

(Received 23 November 2020; revised manuscript received 23 January 2021; accepted manuscript online 1 March 2021)

A method of detecting the single channel triaxial magnetic field information based on diamond nitrogen-vacancy (NV) color center is introduced. Firstly, the incident angle of the bias magnetic field which can achieve the equal frequency difference optically-detected magnetic resonance (ODMR) spectrum of diamond NV color center is calculated theoretically, and the triaxial magnetic information solution model is also constructed. Secondly, the microwave time-controlled circuit module is designed to generate equal timing and equal frequency difference microwave pulse signals in one channel. Combining with the optical detection magnetic resonance technology, the purpose of sequentially locking and detecting the four formant signals on one side of the diamond NV color center ($m_s = -1$ state signal) is achieved, and the vector magnetic field information detection is accomplished by combining the triaxial magnetic information solution model. The system can obtain magnetic field detection in a range of 0 mT–0.82 mT. The system's magnetic noise sensitivity is 14.2 nT/Hz$^{1/2}$, and the deviation angle errors of magnetic field detection θ_x and θ_y are 1.3° and 8.2° respectively.

Keywords: nitrogen-vacancy (NV) color center, vector, electron spin, magnetic detection

PACS: 07.55.Ge, 76.30.Mi, 42.50.Dv **DOI:** 10.1088/1674-1056/abea84

1. Introduction

With the constant development of atomic and quantum physics technology fields, solid-state electron spin has become a research focus in quantum sensing.[1,2] Compared with traditional magnetic measurement techniques such as Hall effect sensor, superconducting quantum interference device (SQUID) magnetometry, and magnetic microscope,[3–6] the method based on the diamond nitrogen-vacancy (NV) color center has exceptional characteristics of sensitivity, volume, power consumption, *etc*.,[7–11] which makes it more extensively applied to weak magnetic measurement technology.[12] It can identify a nanometer-resolved magnetic field at room temperature.[13–15] It is extensively utilized in aerial surveys, marine monitors, earthquake prediction, and medical nuclear magnetic resonance. It is of grand significance in science and technology, military, economy, and other fields.[16]

The unique crystal structure of the NV color center (face-centered cubic structure) makes it feasible to distinguish the magnetic field vector.[17] Theoretically, the magnetic field's measurement with the NV color center ensemble in various axial directions can achieve the measurement of the magnetic field vector information. Yahata *et al*. introduced a vector magnetic field sensing method that utilizes multi-frequency microwave pulses to control four different frequency NV centers simultaneously.[18] This measurement method entails three sets of multi-frequency microwave pulse signals to realize a three-axis vector magnetic field. Jennifer *et al*. introduced a vector magnetic field information solving method for synchronously locking the magnetic field information of the four axes of the NV axis,[19] but this method requires four independent microwave sources to generate modulation signals and solves the magnetic fields of the four axes of the NV color center respectively. The measurement method makes the system more complex due to the use of a complicated vector information calculation method. Also, as there are too many microwave systems in the structure, the instruments' connection is intricate. The microwave power could be lost, leading to the alteration of magnetic field detection sensitivity, thereby affecting the final experimental results.

This paper introduces a single-channel three-axis magnetic field information detection method based on the diamond NV color center. A set of the microwave system can measure the vector magnetic field information. Compared with the conventional three-axis vector magnetic field detection process,

*Project supported by the National Natural Science Foundation of China (Grant Nos. 51635011, 51805493, 51775522, 51727808, and 51922009), the Applied Basic Research Program in Shanxi Province, China (Grant No. 201901D111011(ZD)), the Key Research and Development Program in Shanxi Province, China (Grant No. 201803D121067), the Fund from the Key Laboratory for Information Detection and Processing of Shanxi Province, China (Grant No. ISPT2020-2), the Fund from the Key Laboratory of Shanxi Province, China (Grant No. 201905D121001), and the Shanxi "1331 Project" Key Subjects Construction, China.

†Corresponding author. E-mail: guohao@nuc.edu.cn

‡Corresponding author. E-mail: tangjun@nuc.edu.cn

§Corresponding author. E-mail: liuj@nuc.edu.cn

© 2021 Chinese Physical Society and IOP Publishing Ltd

this solution is simple, straightforward, simplified detection system that reduces the complexity of the system, and the cost of experimental equipment. This method supported by the optical detection magnetic resonance (ODMR) spectrum of the diamond NV color center's resonance peaks with four pairs of equal frequency differences. The microwave time-control circuit detects the four resonance peak frequency points of the ODMR spectrum with equal frequency difference on one side (If there is no special reminder, the "unilateral" mentioned in this paper refers to the signal in the $m_s = -1$ state). Then, the four signals of crystal axis electron spin resonance information are locked and detected in order, and the four signals serve as a single output. The variation of the formant frequency offset of the unilateral electron spin resonance signal of the diamond NV color center can be obtained by adjusting the magnitude of the external magnetic field. Therefore, this method can establish a three-axis magnetic information solution model for the NV color center, thereby obtaining the vector change of the external magnetic field. The system can realize magnetic field detection in a range of 0 mT–0.82 mT, the magnetic noise sensitivity is 14.2 nT/Hz$^{1/2}$, and the deviation angle error of magnetic field detection θ_x and θ_y are 1.3° and 8.2° respectively.

2. Experimental principle

The single-channel triaxial vector magnetic field information detection methodology based on the diamond NV color center is introduced in this paper. The principle of vector detection is presented in Fig. 1. Four pairs of ODMR spectra with equal frequency difference can be obtained by applying an external static magnetic field at a specific angle. They are then utilized as a reference to make the magnetic field measurement benchmark of the diamond NV color center axis and ensure their consistency. Hence, the information about the vector magnetic field change is gathered by detecting the change of formant signal in the different axial directions. In addition, a microwave time-controlled module is designed to create four microwave pulse signals with equal time sequence and time interval through a microwave system. As shown in Fig. 1(a), each microwave pulse signal corresponds to the frequency points of the four formant peaks on one side of the ODMR signal, and the time interval between the adjacent pulse signals is the time difference between the adjacent equal frequency difference ODMR formant signals. Thus, the microwave pulse duration should be greater than the hardware response time, in order to detect and lock the equal frequency difference in the ODMR spectrum for unilateral four formant signals sequentially.

By demodulating the ODMR signal, a demodulation curve can be obtained, and the center frequency of the demodulation curve locks the resonance peak of the ODMR spectrum, the value of the resonance peak signal is taken as the initial value of magnetic field detection. The signal value is fixed and does not change with fluorescence intensity or magnetic field. For a detailed explanation as shown in Ref. [20]. There is a linear region in the process of magnetic field change, making the formant frequency drift Δf_i proportional to the change of the fixed frequency signal ΔU_i as follows:

$$\Delta f_i = k\Delta U_i \quad (i = 1,2,3,4), \tag{1}$$

where k is a constant.

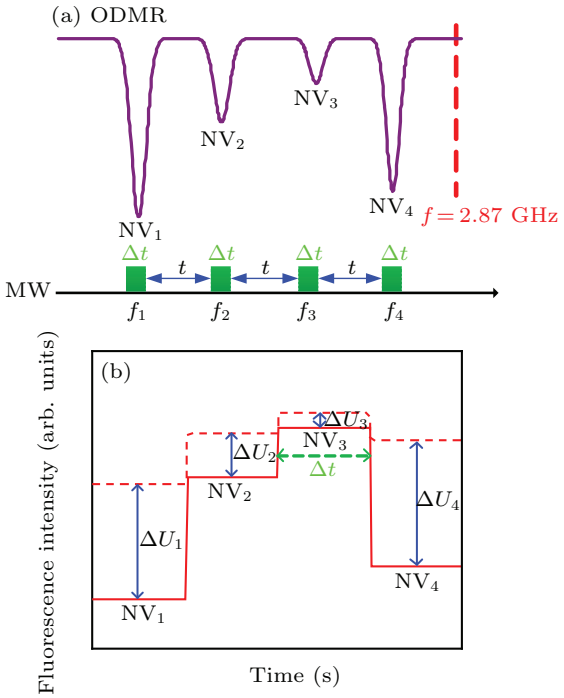


Fig. 1. Principle diagram of single-channel triaxial vector magnetic information detection, showing (a) ODMR signal with equal frequency difference on one side of the diamond NV color center and a single microwave pulse signal (Δt is microwave pulse signal's duration, and t is interval time between adjacent microwave pulse signals), (b) four axial resonance peak signals of the ODMR spectrum detected by microwave timing module, where solid line is the initial four-channel signal, and dotted line is four-channel signal collected after changing the external magnetic field.

With the joint action of microwave timing control circuit and optical detection magnetic resonance technology, the four-channel signals in Fig. 1(b) (solid line) are achieved, which is recorded as the initial value. The duration of each signal is Δt. While adjusting the size of the external magnetic field, the four-channel formant signal collected by the PD also changes accordingly, and the amount of change is ΔU_i $(i = 1,2,3,4)$ as shown in the dotted line in Fig. 1(b).

The magnetic field component of each axis of diamond NV color center ΔB_i can be measured from the following equation:

$$\Delta B_i = \frac{\Delta f_i}{\gamma_e} \quad (i = 1,2,3,4), \tag{2}$$

where γ_e is the gyromagnetic ratio and $\gamma_e = 2.87$ MHz/Gs (1 Gs = 10^{-4} T).

Therefore, the change in voltage ΔU_i at the fixed frequency point of the diamond NV color center ODMR spectrum is proportional to the change in magnetic field ΔB_i as expressed below:

$$\Delta B_i = \frac{k}{\gamma_e}\Delta U_i \quad (i = 1,2,3,4). \tag{3}$$

The variation of magnetic information of triaxial vector $\Delta \boldsymbol{B}$ can be calculated from the following equation:

$$\Delta \boldsymbol{B} = \boldsymbol{A} \cdot \begin{bmatrix} \Delta B_1 \\ \Delta B_2 \\ \Delta B_3 \\ \Delta B_4 \end{bmatrix}, \tag{4}$$

where $\boldsymbol{A}$ is the solution model matrix of the spatial relationship between the four axial magnetic field components of the NV color center and the triaxial vector magnetic field.

3. Experiments and results

3.1. Design of four pairs of magnetic resonance peaks

The spatial coordinate system of the diamond NV color center axis and the three-axis vector magnetic field are established in Fig. 2, where the NV color center principal axis coincides with the Z axis. The external magnetic field $\boldsymbol{B}$ can be expressed by polar angle θ and azimuth ψ. The magnetic field components of the magnetic field $\boldsymbol{B}$ acting on each NV color center axis are represented by B_1, B_2, B_3, and B_4 (corresponding to the diamond axis NV_1, NV_2, NV_3, and NV_4).Therefore, the vector solution model of the axial magnetic field component and the triaxial magnetic field of diamond NV color center is described as follows:

$$\begin{bmatrix} B_X \\ B_Y \\ B_Z \end{bmatrix} = \begin{bmatrix} 0 & \sqrt{2}/3 & \sqrt{2}/3 & -2\sqrt{2}/3 \\ 0 & \sqrt{6}/3 & -\sqrt{6}/3 & 0 \\ 1 & 0 & 0 & 0 \end{bmatrix} \cdot \begin{bmatrix} B_1 \\ B_2 \\ B_3 \\ B_4 \end{bmatrix}. \tag{5}$$

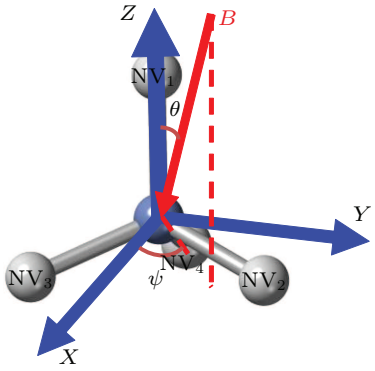


Fig. 2. Definition of Cartesian coordinate system and four NV axes.

After the changes of formant signal in various axial directions of the diamond NV color center are detected by the microwave timing control module, according to the relationship between the variations of formant signals in different axial directions of NV and the magnetic field in the axial direction and the vector solution model of the triaxial magnetic field, the relationship between the variations of formant signal in different axial directions of NV color center and triaxial vector magnetic field can be obtained.

In this paper, three-axis vector magnetic field information measurement method relies on the ODMR spectrum of four pairs of peaks with an equal frequency difference of the diamond NV color center. According to Eq. (2), the magnetic field component difference along the NV axis should be equivalent to the ODMR spectrum with an equal frequency difference, *i.e.*,

$$B_1 - B_2 = B_2 - B_3 = B_3 - B_4. \tag{6}$$

While applying a magnetic field $\boldsymbol{B}$ in any direction to the NV axis, the magnetic field components on the NV axis include

$$\begin{aligned} B_1 &= B\cos\theta - \frac{\sqrt{2}}{4}B\sin\theta\cos\psi - \frac{\sqrt{6}}{4}B\sin\theta\sin\psi, \\ B_2 &= \frac{1}{9}B\cos\theta + \frac{3\sqrt{2}}{4}B\sin\theta\cos\psi + \frac{\sqrt{6}}{2}B\sin\theta\sin\psi, \\ B_3 &= \frac{1}{9}B\cos\theta + \frac{3\sqrt{2}}{4}B\sin\theta\cos\psi, \\ B_4 &= \frac{1}{9}B\cos\theta - \frac{3\sqrt{2}}{4}B\sin\theta\cos\psi + \frac{\sqrt{6}}{4}B\sin\theta\cos\psi. \end{aligned} \tag{7}$$

By substituting Eq. (7) into Eq. (6), the polar angle and azimuth angle can be obtained as follows:

$$\begin{aligned} \theta &= \arctan\left(\frac{8}{9}\cdot\frac{2}{\sqrt{42}}\right) \approx 15.3^\circ, \\ \psi &= \arctan\frac{2}{\sqrt{3}} = 49.1^\circ. \end{aligned} \tag{8}$$

Therefore, when the angle of external bias magnetic field is adjusted to $\theta = 15.3^\circ$ and $\psi = 49.1^\circ$, the ODMR spectrum with equal frequency difference can be obtained, which creates a consistent performance with the magnetic field measurement data of diamond NV axis.

3.2. Construction of experimental system

In this paper, the single-channel triaxial vector magnetic detection process essentially involves the microwave system, the optical system, and the data acquisition and processing system. The microwave system includes the host computer software, the microwave control module, the microwave timing control module, and the microwave source module, which realizes the function of sweeping microwave frequency and the production of equal time sequence and frequency difference microwave pulse signals. The optical system principally comprises a laser (532 nm), microwave antenna, diamond (the electron implantation dose of the diamond sample used in the experiment is 9×10^{18} $e^-\cdot cm^{-2}$, the irradiation energy is 8 MeV, and the concentration is 2 ppm), filter, and optical lens

combination. On this device,the fluorescence detection and microwave control functions of the diamond NV color center are accomplished. The data acquisition and processing system principally includes a photodetector (DET100A2, THORLABS), an oscilloscope (MDO4104C, Tektronix), modulation module and the three-axis magnetic information solution model (data calculation is carried out via PC), and performs the function of the collecting ODMR information of NV color center and solving three-axis magnetic information. The principle of the experimental system is demonstrated in Fig. 3.

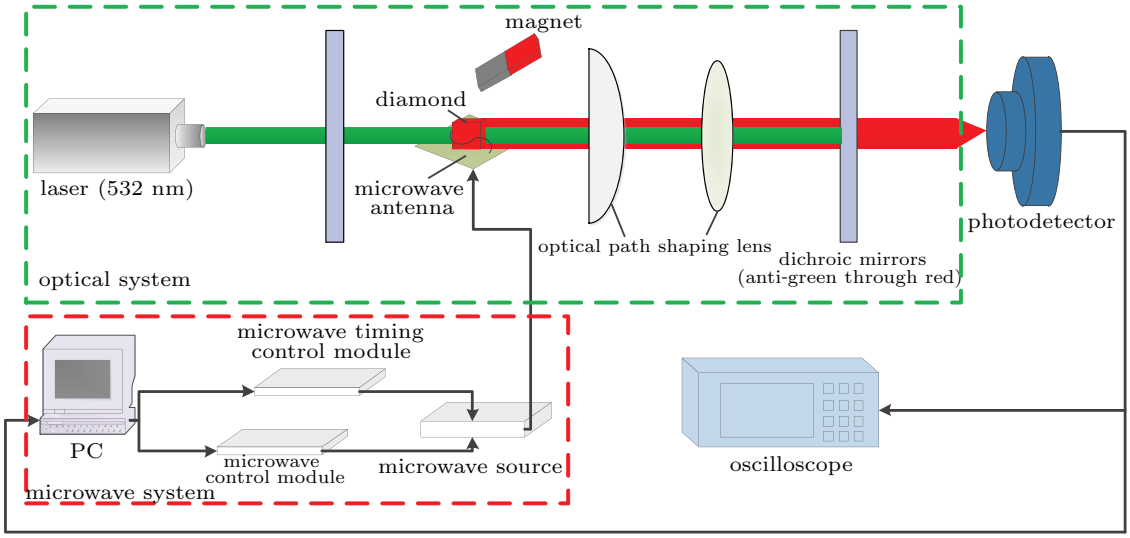


Fig. 3. Schematic diagram of experimental detection.

The microwave timing control module is principally a phase-locked loop control circuit with STM32 as a core. The general phase-locked loop structure comprises a phase detector, a loop filter, a voltage-controlled oscillator (VCO), and a frequency divider. The reference signal is transmitted back from the VCO, and the frequency dividing signal is sent to the phase detector for identification. The phase detector generates an erroneous voltage proportional to the phase difference between the two input signals. After the loop filter identifies the erroneous voltage, only the direct current (DC) component is employed as the tuning voltage of the voltage-controlled oscillator to adjust the oscillation frequency accordingly and hence performing the synchronous phase tracking. Based on the above principle, STM32 and LABVIEW possess significant applications in designing the microwave pulse-signal control circuit board and the host computer-control software. The primary function is the production and output of these four microwave pulse signals with equal timing and frequency difference to detect the single-side four-channel equal frequency difference formant signal of the ODMR spectrum.

3.3. Measurement and characterization of four pairs of magnetic resonance peaks

3.3.1. Experimental process

Use the laser to excite the diamond NV color center to produce red fluorescence. The PC-side host computer commands the microwave-control module to create control signals, and then commands the microwave source to create sweeping information and render it to the microwave antenna in the integrated module (microwave sweep range is 2600 MHz–3100 MHz, step 20 kHz/ms), and act on the diamond to make the fluorescence signal generate the electron-spin resonance peak signal. Then, the photodetector will collect the signal and display it on the oscilloscope and the PC-side host computer.

Adjust the incident angle of the external bias magnetic field to $\theta = 15.3°$, $\psi = 49.1°$. After that, by the magnetic field's size, the ODMR signal with an equal frequency difference of 50 MHz is received as shown in Fig. 4(a). The microwave control module completes the detection of single-sided four-channel equal frequency difference formant signals as shown in Fig. 4(b). These data are recorded as the initial value, and utilized as the benchmark for the magnetic field detection. When the external magnetic field changes, the alteration of the single-sided formant signal of the ODMR is determined and the signal processed by the demodulation module is substituted into the triaxial magnetic information solution model in Eq. (5) to get the current vector change magnetic field (The progress is actualized by PC-based data processing software).

According to the ODMR spectrum with equal frequency difference shown in Fig. 4(a), the resonance frequency values of different axial NV color centers are $f_{\mathrm{NV}_1} = 2699$ MHz, $f_{\mathrm{NV}_2} = 2748$ MHz, $f_{\mathrm{NV}_3} = 2804$ MHz, $f_{\mathrm{NV}_4} = 2849$ MHz. The four frequency points are inputted into the selected computer control software with the microwave time-controlled module. Based on the data, the signal holding time Δt is 2500 ms. The control command is then sent to the circuit

board with the time-controlled module to perform the functionality of four microwave pulse signals with equal frequency difference and equal time sequence, and thus detecting and collecting the resonance peak signals corresponding to the NV color centers in different axes. The detection result is demonstrated in Fig. 4(b), and the detection result is recorded as the initial value.

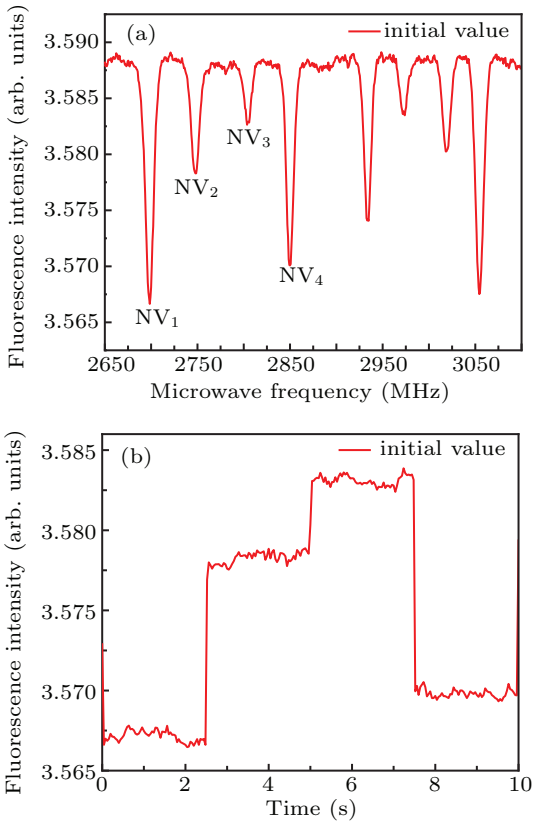


Fig. 4. Initial value detection results, showing (a) ODMR spectrum with equal frequency difference, (b) single-channel output of four formant signals with equal frequency difference.

Based on the Zeeman splitting effect of the diamond NV color center,[21] the formant signal frequency will drift when the external magnetic field is altered. The frequency drift range of the formant signal cannot exceed the width of the single formant signal's absorption peak. Consequently, the detectable magnetic field range of the detection system can be calculated theoretically, according to the formant signal absorption peak's widths in different axial directions in Fig. 4(a). Thus, the maximum magnetic field changes that can be detected in the three axial directions are shown in Table 1.

Table 1. Magnetic field detection range.

Magnetic	*X* axis	*Y* axis	*Z* axis	Total magnetic field
$\Delta B_{\max}$ (mT)	0.39	0.39	0.61	0.82

3.3.2. Measurement and analysis of triaxial magnetic information

Via the three-axis Helmholtz coil, the change of the magnetic field can be guided directionally. The Helmholtz coil used in this experiment is a three-axis coil customized at the 710 Research Institute of China Shipbuilding Industry Corporation. The calibration reveals that the magnetic field transformation amounts of the three-axis Helmholtz coil in the *X*, *Y*, and *Z* axes are 72.9 nT/mA, 61.9 nT/mA, and 63.6 nT/mA. Using the magnetic field on the *Z* axis of the Helmholtz coil as a variable, and applying a current through a digital constant current source to adjust the *Z*-axis magnetic field's magnitude, the strength of the magnetic field varies from 0 μT to 317.4 μT. The changes of frequency drift in the diamond NV color center ODMR spectrum under different magnetic fields are exhibited in Fig. 5(a), and the change of single-channel four-way formant signal processed by demodulation module is exhibited in Fig. 5(b).

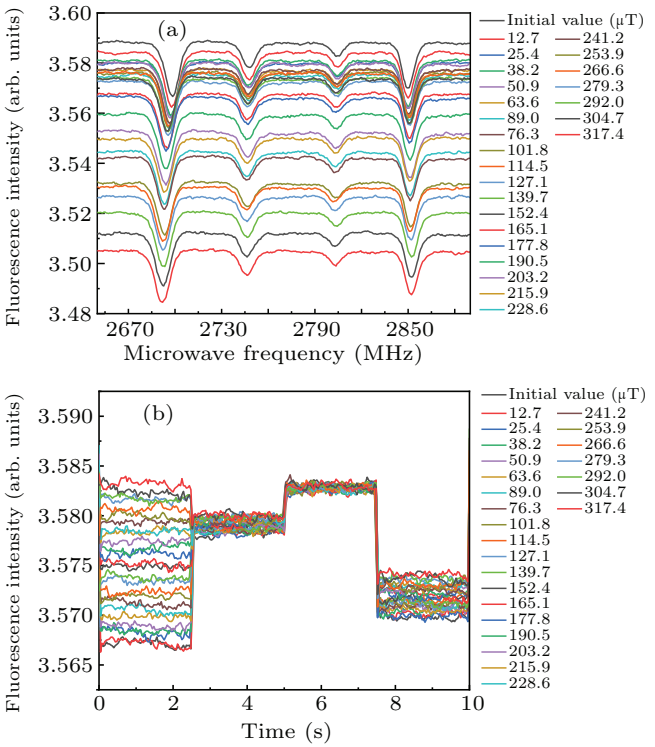


Fig. 5. Changes of ODMR spectrum signal under different magnetic fields: (a) frequency drift and (b) single channel four-channel signal.

According to Fig. 5(b), the single-channel four-channel signal value varies with external magnetic field. Owing to the applied external magnetic field *B* along the *Z* axis corresponding with the NV_1 axis, $B_{NV_1} = B$, $B_{NV_2} = B_{NV_3} = B_{NV_4} = B/3$. The relationship between the magnetic field components on each axis of NV and the voltage value of the fixed frequency signal on that axis can be analyzed, as shown in Figs. 6(a) and 6(b). Consequently , when the magnetic field detection range falls in a range between 0 μT to 317.4 μT, the voltage value of the fixed frequency signal of each axis of the diamond NV color center is proportional to the magnetic field, and the rate between the voltage value of the fixed frequency signal of each axis and the magnetic field is 0.053 mV/μT, 0.017 mV, 0.003 mV/μT, 0.038 mV/μT, separately. The mag-

netic noise power spectral density measured by the lock-in amplifier is shown in Fig. 7. The optical detection magnetic resonance system's magnetic noise sensitivity based on the single-channel three-axis magnetic information detection system is 14.2 nT/Hz$^{1/2}$.

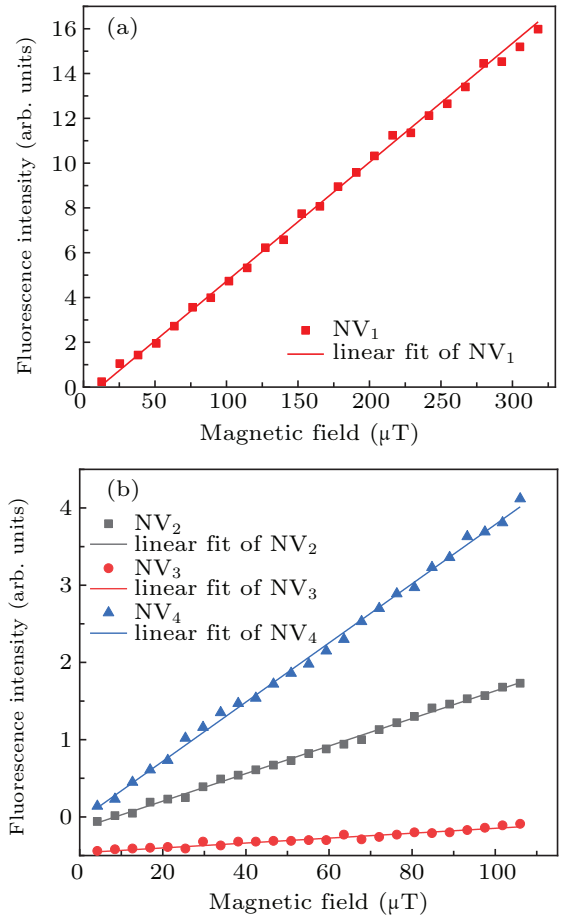


Fig. 6. Changes of formant frequency signals of NV color centers with magnetic field for (a) NV color center NV_1 and (b) NV color center NV_2, NV_3, and NV_4.

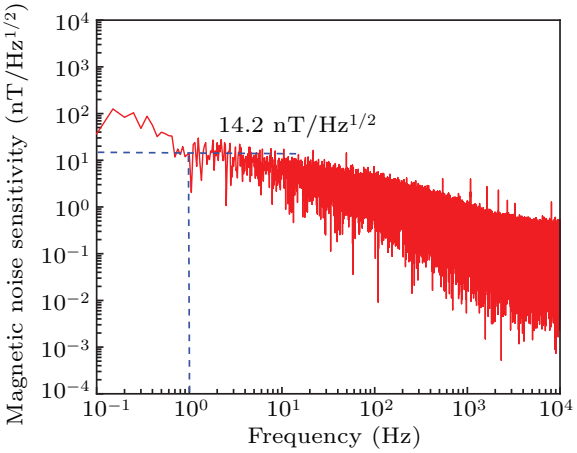


Fig. 7. Magnetic noise spectral density *versus* frequency.

Therefore, by comparing the initial values of the formant signal of each axis of the NV color center, the changes of formant signal in different axial directions and the changes of magnetic field ΔB_i $(i = 1,2,3,4)$ of different diamond NV color center axis can be obtained. Also, the variation of triaxial vector magnetic field B_X, B_Y, and B_Z can be acquired by substituting ΔB_i into the solution relation of triaxial vector magnetic field as shown in Eq. (5). The triaxial magnetic field information captured by this system is shown in Fig. 9(a).

A traditional magnetic field detection method, where a triaxial magnetic sensor is used, is regarded as an exemplar of triaxial orthogonality. However, due to the influence of the diamond sample placement and the installation level of experimental equipment, the magnetic sensor based on the diamond NV color center cannot achieve absolute triaxial orthogonality. Because the principal axis of the diamond NV color center coincides with the Z axis of triaxial magnetic field coordinate system, there appear the deviation angles θ_x and θ_y between the measured triaxial vector magnetic field O-$X'Y'Z$ and the established triaxial vector magnetic field coordinate system O-XYZ as shown in Fig. 8.

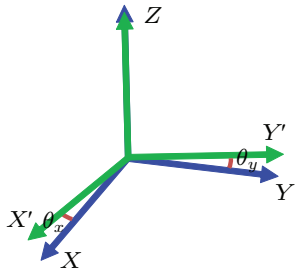


Fig. 8. Schematic diagram of deviation angle in magnetic field detection of diamond NV color center.

When a Helmholtz coil is employed to create a magnetic field in the Z axis, theoretically, only the magnetic data on the Z axis will changes accordingly. However, there is a deviation between the magnetic field on the X axis and the magnetic field on the Y axis as shown in Fig. 9(b). The magnetic field deviation angle θ_i can be calculated from the the following equation:

$$\theta_i = \frac{\pi}{2} - \arccos\frac{B_i}{B}, \tag{9}$$

where B_i is the magnetic field deviation value in each axial direction, and B is the applied external magnetic field. Selecting the maximum deviation magnetic field value on the X axis and the Y axis, the maximum deviation angle on the X axis and the Y axis are calculated to be 1.3° and 8.2°, respectively.

Consequently, the experimental results can demonstrate that the single-channel three-axis magnetic information detection method proposed in this paper can achieve the purpose of measuring three-axis vector magnetic information. This method can perform the detection of magnetic vector information by utilizing a microwave system. It resolves the problem that three independent detection systems are required in the conventional three-axis vector magnetic detection method, it avoids the problem of large measurement error caused by three independent processes and simplifies the three-axis magnetic information detection system.

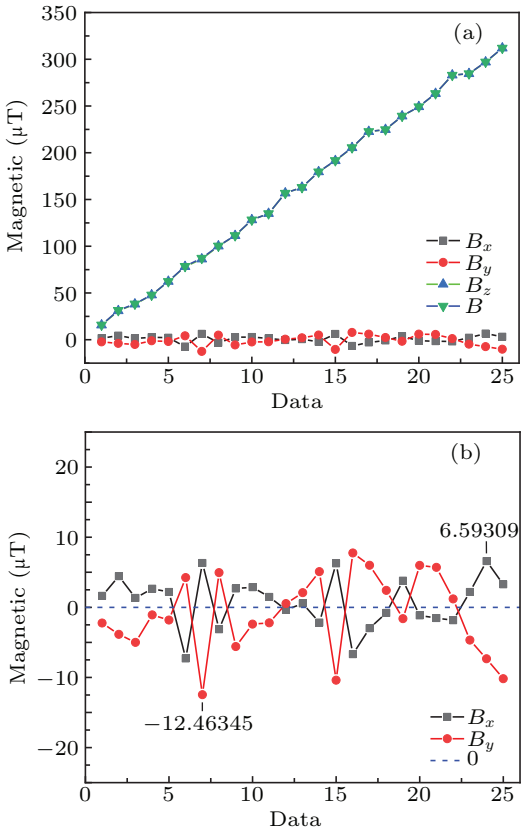


Fig. 9. Three-axis magnetic field solution results. (a) Magnetic field data calculated by three-axis vector solution model; (b) magnetic field data on the X axis and Y axis.

4. Conclusions

This paper introduces a single-channel three-axis vector magnetic information detection that employs diamond NV color center. A microwave system is used to detect the three-axis magnetic information. The function of single-channel acquisition and measurement of these diamond NV color center formant signals on different axes is accomplished. Then the vector magnetic field detection is also performed. In this paper, a particular angle is calculated theoretically, and the equal frequency difference ODMR spectrum is obtained, which is adopted as a benchmark for magnetic field detection. A microwave time-controlled module is designed to achieve the single-channel detection of unilateral four-channel formant signals in the ODMR spectrum, obtain the unilateral formant signal offset under the unknown magnetic field and the magnetic field information in different axes of NV. A triaxial vector magnetic information solution model is hence established. The informatin about vector variation of the external magnetic field is obtained by determining the relationship between the different axial magnetic field components of the diamond NV color center and the triaxial vector magnetic field. The system can well detect the magnetic field in a range of 0 mT–0.82 mT, the magnetic noise sensitivity is 14.2 nT/Hz$^{1/2}$, and the deviation angle error of magnetic field detection θ_x and θ_y are 1.3° and 8.2° respectively. This novel detection method could serve as a high-precision magnetic navigation platform and magnetic shielding compensation technology.

References

[1] Barry J F, Schloss J M, Bauch E, Turner M J, Hart C A, Pham L M and Walsworth R L 2020 *Rev. Mod. Phys.* **92** 015004
[2] Shang Y X, Hong F, Dai J H, Yu H, Lu Y N, Liu E K, Yu X H, Liu G Q and Pan X Y 2019 *Chin. Phys. Lett.* **36** 086201
[3] Espitia M G M 2014 *Journal of the Microelectronic Engineering Conference* **20** 34
[4] Seltzer S J and Romalis M V 2004 *Appl. Phys. Lett.* **85** 4804
[5] Gudoshnikov S, Tarasov V, Liubimov B, Odintsov V, Venediktov S and Nozdrin A 2020 *J. Magn. Magn. Mater.* **510** 166938
[6] Zhang S L and Cao N 2020 *Chin. Phys. B* **29** 40702
[7] Liao Q H, Ye Y, Li H Z and Zou N R 2018 *Acta Phys. Sin.* **67** 040302 (in Chinese)
[8] Guo H, Gao Y J, Qin Y, Wang S X, Liu Y S, Zhang Z R, Li Z H, Wen H F, Tang J, Ma Z M, Li Y J and Liu J 2021 *Nanotechnology* **32** 055502
[9] Wang C J, Shi F Z, Wang P F, Duan C K and Du J F 2018 *Acta Phys. Sin.* **67** 130701 (in Chinese)
[10] Perunicic V S, Hall L T, Simpson D A, Hill C D and Hollenberg L C L 2014 *Phys. Rev. B* **89** 054432
[11] Balasubramanian G, Neumann P, Twitchen D, Markham M, Kolesov R, Mizuochi N, Isoya J, Achard J, Beck J, Tissler J, Jacques V, Hemmer P R, Jelezko F and Wrachtrup J 2009 *Nat. Mater.* **8** 383
[12] Zhao L, Yue D H, Liu C L, W M, Han Y H and Gao C X 2019 *Chin. Phys. B* **28** 030702
[13] Wang P f, Ju C Y, Shi F Z and Du J F 2013 *Chin. Sci. Bull.* **58** 2920
[14] Geiselmann M, Juan M L, Renger J, Say J M, Brown L J, de Abajo F J G, Koppens F and Quidant R 2013 *Nat. Nanotechnol.* **8** 175
[15] Blank A, Shapiro G, Fischer R, London P and Gershoni D 2015 *Appl. Phys. Lett.* **106** 034102
[16] Eismont N, Klas J and Shimonek J 1994 *Journal of the Brazilian Society of Mechanical Sciences* **16** 32
[17] Zhao B B, Guo H, Zhao R, Du F F, Li Z H, Wang L, Wu D J, Chen Y L, Tang J and Liu J 2019 *IEEE Magn. Lett.* **10** 8101104
[18] Yahata K, Matsuzaki Y, Saito S, Watanabe H and Ishi-Hayase J 2019 *Appl. Phys. Lett.* **114** 022404
[19] Schloss J M, Barry J F, Turner M J and Walsworth R L 2018 *Phys. Rev. Appl.* **10** 034044
[20] Deng S L, Zhang W D, Guo H, Wu D J, Li Z H, Wen H F, Tang J, Han X C, Ma Z M, Liu J and Li Y J 2020 *Laser Phys. Lett.* **17** 105205
[21] Hanzawa H, Nishikori H, Nisida Y, Sato S, Nakashima T, Sasaki S and Miura N 1993 *Physica B* **184** 137